Environmental Research 268 (2025) 120750

Contents lists available at ScienceDirect

Environmental Research

journal homepage: www.elsevier.com/locate/envres

Polystyrene microplastics exhibit toxic effects on the widespread coral symbiotic *Cladocopium goreaui*

Jiayuan Liang [a,*,1], Tianyi Niu [a,d,1], Li Zhang [c], Yating Yang [a], Zhicong Li [a], Zhuqing Liang [a], Kefu Yu [a,b,**], Sanqiang Gong [a]

[a] Guangxi Laboratory on the Study of Coral Reefs in the South China Sea, School of Marine Sciences, Guangxi University, Nanning, 530004, China
[b] Southern Marine Science and Engineering Guangdong Laboratory (Guangzhou), Guangzhou, 510030, China
[c] School of Resources, Environment and Materials, Guangxi University, Nanning, 530004, China
[d] State Key Laboratory of Urban and Regional Ecology, Research Center for Eco-Environmental Sciences, Chinese Academy of Sciences, Beijing, 100085, China

ARTICLE INFO

Keywords:
Microplastics
Coral reef ecosystem
Symbiodiniaceae
Photosynthesis
Energy metabolism

ABSTRACT

Within the coral reef habitat, members of the Symbiodiniaceae family stand as pivotal symbionts for reef-building corals. However, the physiological response of Symbiodiniaceae on microplastics are still poorly understood. Research conducted in this investigation assessed the harmful impact of polystyrene microparticles (PS-MPs) on *Cladocopium goreaui*, a Symbiodiniaceae species with a broad distribution. The results showed that micrometre-sized PS-MPs had a greater toxic effect on *C. goreaui* than nanometre-sized PS-MPs, and the growth inhibition rate of a concentration of 20 mg/L with 10 μm-sized PS-MPs on *C. goreaui* was as high as 62.9%–86%, which almost completely inhibited cell proliferation. Exposure to 10 μm PS-MPs significantly increased cell damage, for instance, the concentration of extracellular polymeric substance and malondialdehyde have increased by 161.6%–184.4% and 261.8%–896% on days 10–20 respectively. Furthermore, When PS-MPs inhibited the photosynthesis of *C. goreaui*, it could ensure their typical photosynthetic activity maintained by increasing their chlorophyll levels, and the increase in chlorophyll concentration is proportional to the level of inhibition experienced. However, Exposure to 10 μm PS-MPs could damage the chloroplasts of *C. goreaui*, leading to a decrease in the ability to synthesize photosynthetic pigments and subsequently resulting in a reduction in photosynthetic capacity. The morphology and genetic activity of *C. goreaui* suggest that PS-MPs primarily induce cellular shrinkage and distortion, as well as the disintegration and impairment of nuclear and chloroplastic structures, concurrently eliciting a greater number of suppressed genes, predominantly those associated with the function of succinate dehydrogenase, the attachment to tetrapyrroles, the binding of haem, and the handling of iron ions, including activities related to oxidoreduction. The investigation examined the adverse impacts of PS-MPs on a crucial coral symbiont (Symbiodiniaceae) and the beneficial reaction of these algal organisms, enhancing comprehension of how microplastic pollution affects the coral reef ecosystem.

1. Introduction

Coral reefs showcase significant levels of primary productivity alongside a rich variety of biodiversity (Mooney et al., 2009; Hoegh--Guldberg, 2011). Although coral reefs occupy only approximately 0.25% of the global marine area, they provide habitat for nearly 30% of marine organisms and are known as "tropical rainforests of the sea" (Reaka-Kudla and L, 1997; Yu, 2018). The continuous decline in the health of coral reef habitats is intensifying as a result of issues including climate change, excessive fishing practices, and the contamination of the natural environment (Hughes et al., 2003; Yu, 2012). With societal development, plastic pollution and that of its additives have become serious threats to Earth's ecosystems (Jambeck et al., 2015; Sendra et al., 2021). In the natural environment, plastic waste is gradually decomposed into small particles through physical, chemical, and biological processes, forming microplastics (MPs) with diameters less than 5 mm

* Corresponding author.
** Corresponding author. Guangxi Laboratory on the Study of Coral Reefs in the South China Sea, School of Marine Sciences, Guangxi University, Nanning, 530004, China.
E-mail addresses: jyliang@gxu.edu.cn (J. Liang), kefuyu@scsio.ac.cn (K. Yu).
[1] These authors contributed to the work equally and should be regarded as co-first authors.

https://doi.org/10.1016/j.envres.2025.120750
Received 5 November 2024; Received in revised form 22 December 2024; Accepted 1 January 2025
Available online 2 January 2025

(Thompson et al., 2004; Lambert et al., 2013; Auta et al., 2017; Yang et al., 2020). And after secondary decomposition, nanoplastics with particle size less than 100 nm can be formed (Sana et al., 2020). MPs are widely distributed, including in rivers, soil, oceans, and even the air (Li et al., 2021a, b; Zhou et al., 2021). It is estimated that more than 8 million tons of plastic waste enter the ocean from land each year and are dispersed to every corner of the ocean by ocean currents (Schwarz et al., 2019; Van Sebille et al., 2020). This has led to the ubiquitous threat of MPs pollution in coral reefs. MPs have been detected in coral reef areas such as the Great Barrier Reef in Australia (Jensen et al., 2019), the Maldives archipelago (Imhof et al., 2017; Saliu et al., 2018), and numerous islands in the South China Sea (Ding et al., 2019a; Huang et al., 2019). MPs in coral reef ecosystems can be ingested by reef-dwelling organisms in different ways, thereby entering the food chain cycle and being difficult to degrade (Wright et al., 2013; Ivleva et al., 2017). Rotjan et al. (2019) analysed different coral species on Rhode Island and detected many MPs in each polyp, with an average content of more than 100. Simultaneously, in indoor experiments, it was found that when polyethylene MPs (107.5–230.8 μm) and brine shrimp eggs of similar size coexisted, the coral *Astrangia poculata* preferred to ingest MPs and exhibited a certain resistance response to brine shrimp eggs, indicating that corals would inhibit their intake of other foods after ingesting MPs. Tang et al. (2018) have found that short-term contact with PS-MPs provokes a stress reaction within the scleractinian coral species *Pocillopora damicornis*, which activates the JNK and ERK signalling pathways. This activation impairs the coral's fungal detoxification and defense mechanisms, consequently diminishing its ability to resist stress and compromising its immune function.

Reef-building corals are typical symbiotic organisms that are composed of coral polyps and various microorganisms, such as Symbiodiniaceae, bacteria, fungi, viruses, and protozoa, that form a "holobiont" in a mutualistic symbiotic relationship (Wegley et al., 2007; Robbins et al., 2019). In tropical and subtropical coral reef environments, Symbiodiniaceae constitute the predominant group of symbiotic phototrophs (Su et al., 2020). The partnership between these microorganisms and reef-building corals forms the foundation of coral reef ecosystems, due to the fact that the energy produced through photosynthesis by Symbiodiniaceae fulfills up to 95% of the nutritional needs of the corals they inhabit (Houlbrèque and Ferrier-Pagès, 2009; González-Pech et al., 2019).The family Symbiodiniaceae comprises several distinct clades, such as *Symbiodinium* (Clade A), *Breviolum* (Clade B), *Cladocopium* (Clade C), *Durusdinium* (Clade D), and *Fugacium* (Clade F) (LaJeunesse et al., 2018). As identified by Gong et al. (2021) with *Cladocopium* and *Durusdinium* being dominant in tropical Indo-Pacific corals. The Cladocopium genus is the most diverse genus of Symbiodiniaceae, and *C. goreaui* is the most representative species. It has high photosynthetic efficiency, which can help coral hosts tolerate seasonal low temperature and high nutrient environments (Baker et al., 2013). Symbiotic dinoflagellates play a key role in coral bleaching, therefore, they are often used as important indicators of coral health. MPs not only inhibit the photosynthesis of phytoplankton but also cause direct physical damage to algae (Ding et al., 2019b). Microparticle contaminants in marine environments vary in dimension from several nanometers to hundreds of micrometers, with their harmful impacts being intimately linked to the scale of the particles. Chen et al. (2020) found that after exposure to MPs of different sizes at the micrometre level for 72 h, *Scenedesmus quadricauda* and *Platymonas helgolandica* var. *tsingtaoensis*, two types of microalgae, contained 1–2 μm diameter MPs in some cells, with a significant decrease in microalgal density and inhibition of photosynthesis; however, MPs with a diameter of 3–5 μm were not found inside the cells. Moreover, Xiao et al. (2020) reported that at a concentration of 10 mg/L, the toxicity of 5 μm diameter MPs to the freshwater microalga *Euglena gracilis* was greater than that of 0.1 μm diameter MPs. These MPs not only inhibited algal cell growth but also reduced the content of photosynthetic pigments and increased SOD activity. In the study by Cao et al. (2022b),1 μm MP had a significantly greater inhibitory effect on the growth of the freshwater alga *Chlorella pyrenoidosa* than 5 μm MP did, also significantly reducing the content of photosynthetic pigments, inducing an oxidative stress response in cells, and damaging the integrity of cell membranes. The varied outcomes demonstrate that analyses of MPs' influence on microalgae should encompass not just the adverse impacts of uniform-sized particles but also the collective toxicity stemming from a range of MPs sizes. Regarding the toxicity of MPs to Symbiodiniaceae, Marangoni et al. (2022) reported that 20 nm PS-MPs reduced the maximum electron transfer rate and total antioxidant capacity of *Symbiodinium* (Clade A) and increased lipid peroxidation. Ripken et al. (2020)'s study indicated that exposure to nanoscale MPs (42 nm) resulted in the upregulation of genes associated with *Cladocopium* sp.(clade C) involvement in motor protein movement and the downregulation of genes related to photosynthesis, mitosis, and intracellular degradation, with more genes being downregulated than upregulated. Research by Su et al. (2020) showed that exposure to 1 μm MP at 5 mg/L suppressed the detoxification activity, nutrient absorption, and photosynthesis of *C. goreaui* observed that elevated oxidative stress and enhanced cellular apoptosis by stimulating ion transport. At present, studies concerning the impact of MPs on Symbiodiniaceae have predominantly focused on minute fragments (20 nm, 42 nm, and 1 μm), while the toxicological consequences of MPs varying in particle size and concentration remain unexplored.

The initiation of the symbiotic partnership termed "coral-Symbiodiniaceae symbiosis" occurs via horizontal transmission for most species that construct coral reefs, according to Ali et al. (2019). Planktonic larvae are important during the early development of corals, and they must absorb free-living Symbiodiniaceae from the environment to form a "coral-Symbiodiniaceae" symbiont (Ng et al., 2019). The peril that MPs pose to Symbiodiniaceae has a direct impact on the wellbeing and equilibrium of the whole coral reef ecosystem. In order to further investigate the toxic mechanism of MPs on Symbiodiniaceae, this study conducted a short-term indoor acute exposure experiment to MPs to study the physiological and biochemical changes and transcription products of *C. goreaui*. Some research had shown that the main types of MPs in the western Pacific Ocean are PP, PVC, PS, and PE (Cui et al., 2022); The main types of MPs in the eastern Indian Ocean are PP, PE, PVC, PS, and PET (Li et al., 2021a, b); The main types of MPs in the Persian Gulf waters are PE, PS, PP (Kor and Mehdinia, 2020). So, this research delved into how various amounts and dimensions (microplastic grade) of polystyrene—among the most prevalent commercial plastics globally—affect the Symbiodiniaceae family detrimentally, examining the underlying processes. Insights garnered from this investigation are anticipated to enhance comprehension of how pivotal coral-associated microbes react to MPs pressures and the implications of these interactions for coral reef environments and further evaluate the potential impact of microplastic pollution on the entire coral reef ecosystem.

2. Materials and methods

2.1. Cultivation of the C. goreaui strain and experimental reagents

The *C. goreaui* strain used in this study was isolated and cultured from Acropora pruinosa on Wuzhou Island, northern South China Sea (Qin et al., 2023). *C. goreaui* was grown in L1 marine water mixture, featuring a 35 parts per thousand saline content, ambient warmth of 25 °C with a 1-degree margin, 90 μmol per square meter per second of luminance, and a photoperiod of 14 h illuminated to 10 h unlit. Using artificial plastic microbeads to simulate the environment can better control experimental conditions, observe the impact characteristics of MPs under different conditions, and more accurately evaluate their potential impact on coral reef environments. In addition, it also can help researchers understand the response patterns of MPs under specific environmental conditions, providing scientific basis for environmental protection and risk assessment. PS-MPs were procured from Tianjin Besttech Research Center, located in Tianjin, China, and were preserved

in suspension form at a concentration of 2.5% by weight to volume in a 10-mL solution. PS-MPs were uniformly dispersed in water and did not precipitate or accumulate during the cultivation experiments.

2.2. MPs exposure experiment

Owing to the steady breakdown and diminishment of plastic within nature, it becomes undetectable when it falls below a specific threshold. So this study selected a wide range of concentrations of MPs from 0 to 50 mg/L and a size range of MPs from 100 nm to 10 μm. *C. goreaui* was cultured to a density of 1.0×10^5 cells/mL. Six groups were set up with different concentrations of 1 μm PS-MPs, 0 mg/L, 2 mg/L, 5 mg/L, 10 mg/L, 20 mg/L, and 50 mg/L, with three replicates per group. The concentration of PS-MPs was fixed at 20 mg/L, and five experimental groups with different particle sizes of 0.1 μm, 0.4 μm, 1 μm, 5 μm, and 10 μm were set up, with three replicates per group. This study selected a particle size range of 0.1–10 μm, ranging from small particle size to particle size similar to *C. goreaui* cells (9.8 ± 1.3 μm) (Qin et al., 2023), to comprehensively explore the toxic effects of microplastic particle size on *C. goreaui*. The particle size was set to 1 μm (the middle value of the particle size range) to investigate the toxicity of MPs at different concentrations, and had good radiation effect on both extreme values on both sides. Setting up a high concentration simulation environment is beneficial for better controlling experimental conditions, observing the impact characteristics of MPs under different conditions, and thus more accurately evaluating their potential impact on coral reef environments. In addition, a high concentration simulated environment helps to enhance the cumulative effect of convex MPs and assists researchers in understanding the response patterns of MPs under specific environmental conditions, providing scientific basis for environmental protection and risk assessment. Therefore, set the concentration range to 0–50 mg/L, and when exploring the toxic effects of MPs with different particle sizes, set the concentration to 20 mg/L. The cultivation conditions were the same as those mentioned above.

2.3. Sample processing and data analysis

2.3.1. C. goreaui growth rate analysis

Samples were taken at 0, 5, 10, and 20 days of culture for analysis and testing. One millilitre of sample solution was removed and fixed with 100 μL of formaldehyde reagent. Cell quantification was performed with a haemocytometer while utilizing a Nikon ECLIPSE Ni-E upright light microscope. Subsequently, the recordings of this data enabled the determination of both cell concentration and proliferation velocity. To compute these parameters, the equation utilized was: Proliferation velocity (μ) = ln(N2/N1)/(t2-t1), wherein μ represents the proliferation velocity (per day), and N2 and N1 signify the respective cellular concentrations (cells/mL) at the distinct time points t2 and t1.

2.3.2. Determination of the photosynthetic pigment content and photobiological efficiency of C. goreaui

Samples were taken at 0, 2, 5, 10, and 20 days of culture for analysis and testing. A 5 mL aliquot of the test liquid was pipetted into a centrifuge tube, then spun at a temperature of 4 °C and a force of 5000×*g* for a duration of 5 min. Following this, the clear liquid above the sediment was discarded, and the residue was treated with 1 mL of methanol. The sample was thoroughly mixed with a vortex mixer, covered in aluminum foil, and stashed away from light at a temperature of 4° Celsius for a full day to allow for the extraction of the photosynthetic pigments. A Varioskan™ LUX multifunctional microplate reader (Thermo Scientific) was used to measure optical density (OD) at 480, 510, 630, 664, and 750 nm wavelengths (Ritchie, 2006; Sun, 2020) in the dark. The photosynthetic pigment content was normalized to the single-cell content (pg/cell). The formulas for determining Chl a, Chl c, and carotenoid levels are as follows:

$$\text{Chlorophyll a } (\mu g/\text{ml}) = 13.6849 \times (OD_{664} - OD_{750}) - 3.4551 \times (OD_{630} - OD_{750})$$

$$\text{Chlorophyll c } (\mu g/\text{ml}) = -7.014 \times (OD_{664} - OD_{750}) + 32.9371 \times (OD_{630} - OD_{750})$$

$$\text{Carotenoids } (\mu g/\text{ml}) = 7.6 \times (OD_{480} - OD_{750}) - 1.49 \times (OD_{510} - OD_{750})$$

The *C. goreaui* cells were incubated in a dark setting for half an hour before their photosystem II (PS II) peak photochemical efficiency, denoted as Fv/Fm, was quantified using a WALZ brand PAM device from Germany.

2.3.3. Determination of extracellular polymeric substance content

Samples were taken at 0, 10, and 20 days of culture for analysis and testing. The quantity of extracellular polymeric substance (EPS) (The main component is exopolysaccharide) was determined through the phenol-sulfuric acid technique as described by Li et al. (2022) and Yue et al. (2022). For this process, the specimen underwent a thermal phase of 80° Celsius lasting 30 min prior to being spun at a force of 8000×*g* for a duration of 10 min at a temperature of 4 °C. From the clarified liquid, a volume of 2 mL was extracted, to which was then introduced 1 mL of phenol at a 6% concentration within a chilled environment. Subsequently, a measured 5 mL of sulfuric acid was incrementally dispensed, taking care to minimize or eliminate thermal emission. Subsequent to the initial procedure, the concoction underwent a boiling process within a water bath for a duration of 20 min, followed by a chilling period in an ice bath spanning 10 min. The OD was then ascertained at a 490 nm wavelength. For calibration purposes, a glucose solution served as the reference. A series of ten varying concentrations (0, 10, 20, 30, 40, 50, 60, 70, 80, and 90 μg/mL) were systematically prepared to establish a concentration gradient. From each level of this gradient, a volume of 2 mL was sampled, and the OD for each was gauged at a 490 nm wavelength, adhering to the procedures previously described.A calibration curve, showing concentration along the horizontal axis and OD vertically, was used to determine the sample's EPS levels, which were then adjusted based on individual cell quantities.

2.3.4. Evaluation of dissolved protein levels, malondialdehyde quantities and superoxide dismutase functionality

Samples were taken at 0, 10, and 20 days of culture for analysis and testing. A volume of 20 mL of the test fluid underwent centrifugation at a temperature of 4 °C and a force of 3000×*g* for a duration of 10 min. Following the extraction of the clear fluid above the sediment, the precipitate was reconstituted with 1.5 mL of Phosphate Buffered Saline and then relocated into a centrifuge tube with a capacity of 2 mL. Then,100 μL of 0.5 mm zirconia grinding beads was added. A mechanical device for tissue homogenization (manufactured by Shanghai Jingxin) facilitated the pulverization process, operating in cycles of 10 s on, 30 s off, totalling six cycles, with the apparatus's adapter precooled in a freezer set to minus 20 °C prior to its application. Following homogenization, the samples were spun at a force of 3000×*g* and a temperature of 4 °C for a duration of 10 min, subsequent to which the clear liquid above the settled particles was extracted. To quantify the amount of dissolvable protein present, an assay kit specifically designed for bicinchoninic acid (BCA) protein analysis (procured from Shanghai Shenggong, China) was employed. The enzymatic function of Superoxide dismutase (SOD) was quantified with the employment of a specific SOD detection kit (A001, Nanjing Jiancheng, China), while the level of malondialdehyde (MDA) was ascertained utilizing a corresponding MDA measurement kit (A003, Nanjing Jiancheng, China). The results were normalized to the single-cell content.

2.3.5. Ultrastructural analysis

Three particle size groups with significant differences, namely 0.1 μm, 1 μm, and 10 μm, were selected for ultrastructural analysis.

2.3.5.1. SEM analysis. Twenty days into the experiment, a 50 mL sample of *C. goreaui* cells was harvested and subjected to centrifugation at 4 °C and at a force of 5000×*g* for a duration of 10 min, subsequently discarding the supernatant. The cells were then rinsed thrice using PBS (0.1 M, excluding NaCl). A 2.5–3% solution of glutaraldehyde, chilled to 4 °C, was introduced to the cells for fixation over a period of 4 h at the same temperature. Following fixation, the preserving agent was eliminated, and the samples underwent a quintuple wash with PBS (0.1 M, NaCl omitted) for 15 min per wash. Subsequent to the attachment of the specimens to the slides, a sequential dehydration was conducted using a range of ascending alcohol concentrations (30%, 50%, 70%, 80%, 90%, 95%, 100%). The alcohol solution was added once for 15 min each, after which the samples were thoroughly dehydrated with 100% alcohol twice for 10 min each. Subsequently, a critical point dryer (Leica EM CPD300) was used for drying treatment. Finally, an ion sputtering coating instrument (Leica EM ACE200) was used to vacuum spray the samples, which were observed through scanning electron microscopy (SEM; HITACHI SU-8010).

2.3.5.2. TEM analysis. On experiment day Twenty, a 50 mL sample of the algal population was harvested, followed by a centrifugation process at 5000×*g* for a duration of 10 min at a temperature of 4 °C. Subsequently, the overlaying liquid was discarded. The collected cells were then stabilized using glutaraldehyde. After being submerged in 0.1M phosphate-buffered saline, the stabilized algal cells were subjected to a triple rinse. The samples were again centrifuged under the same conditions to eliminate any remaining supernatant, with each rinse lasting 20 min. The cells were then treated with 1% osmic acid while maintained at a cool 4 °C, solidified at this temperature for a period between 2 and 3 h, and finally, they were washed with 0.1M PBS three times, allotting 20 min for each washing session. After dehydration with a series of gradient alcohols (30%, 50%, 70%, 80%, 85%, 90%, 95%, 100%), each concentration of alcohol was used once for 15 min each time, after which the samples were thoroughly dehydrated with 100% alcohol twice for 10 min each. Subsequently, used the penetrant to infiltrate, and the penetrant is a mixture of 2 times acetone and 1 time epoxy resin, a mixture of acetone and epoxy resin in equal proportions, and epoxy resin, each at 37 °C overnight in an incubator. Ultimately, the permeated specimen was positioned within a compact container, followed by the incorporation of an embedding medium of epoxy resin, after which the specimen underwent a curing process at a temperature of 60 °C for a duration of 48 h. After curing, the sample was trimmed to a suitable size and shape and sliced on an ultrathin sectioning machine (EM UC7) with a thickness of approximately 60–100 nm. Following the application of lead and uranium as contrasting agents, the specimens underwent examination using a Tecnai G220 TWIN transmission electron microscope (TEM).

2.4. Extraction and sequencing of transcription products

The transcription products were analysed for experimental samples with significant physiological index effects. On day 20 of the stress trial, we gathered and preserved the *C. goreaui* cells from test cohort of control, 1 μm-10 mg/L, 1 μm-20 mg/L, 1 μm-50 mg/L, and 10 μm-20 mg/L by immersing them in liquid nitrogen for a duration of 30 min. The samples were subsequently sent to Shanghai Meiji Biomedical Technology Co., Ltd., for transcriptome sequencing analysis (see Supplementary File S1 for specific methods).

2.5. Statistical analysis

Statistical evaluation was conducted through the application of SPSS, with p-values below 0.05 marking the threshold for statistical relevance. Subsequent examinations of datasets exhibiting notable disparities were carried out utilizing Tukey's post hoc analysis. Figures were generated employing Origin software. Data representation took the form of the mean ± the standard error.

3. Results

3.1. Physiological effects of PS-MPs exposure on C. goreaui

3.1.1. Growth ratios

Fig. 1 illustrates how varying amounts and sizes of PS-MPs particles influence *C. goreaui* cell's development. The particle diameter of PS-MPs was a stronger deterrent to the proliferation rate of *C. goreaui* compared to the quantity. *C. goreaui* cell's expansion was not notably impacted by PS-MPs particles measuring 1 μm C. *goreaui* at different concentrations (0–50 mg/L). However, at a concentration of 20 mg/L, PS-MPs particles 5 μm and 10 μm in size more significantly inhibited the growth of *C. goreaui*. On the 5th, 10th, and 20th days, compared with those in the control group, the growth rates of *C. goreaui* exposed to 5 μm PS-MPs decreased by 22.9%, 22.8%, and 28.8% in these three days respectively. And the growth rates of *C. goreaui* exposed to 10 μm PS-MPs decreased by 62.9%, 86%, and 81.9% in these three days respectively. In particular, PS-MPs with a particle size of 10 μm almost completely inhibited the growth of the cells.

3.1.2. Photosynthesis

During experiments involving various concentrations and sizes of PS-MPs particles, the photochemical efficiency (Fv/Fm) of *C. goreaui* remained stable, except for that of the 10 μm-20 mg/L exposure group, which showed significant inhibition starting from the 5th day (19.5% decrease compared to the control group); moreover, no Fv/Fm values were detected starting from the 10th day (Fig. 2A and B). Photosynthetic pigments are crucial for maintaining photosynthesis. After exposure to different concentrations of PS-MPs with a particle size of 1 μm, a positive correlation was observed on the Chl a content of *C. goreaui*, and in the 1 μm-50 mg/L group, the Chl a content significantly increased beginning on the 5th day (Fig. 2C). When exposed to PS-MPs at size of 5 μm and 10 μm at a concentration of 20 mg/L, the Chl a content of *C. goreaui* significantly increased beginning on the 2nd day and then noticeably decreased on the 10th day (Fig. 2D). When exposed to PS-MPs at particle sizes of 0.1 μm, 0.4 μm, and 1 μm at a concentration of 20 mg/L, the Chl a content of *C. goreaui* significantly increased only on the 20th day ($p < 0.05$). The changes in the Chl c and carotenoid contents were similar to those in the Chl a content (Fig. 2E, F, G, H). The 0.1 μm, 0.4 μm, and 1 μm particles at concentrations of 10–20 mg/L had significantly greater carotenoid contents on the 5th day than did the control group (Fig. 2G and H).

3.2. Impacts of PS-MPs interaction on antioxidant response and cellular protection mechanisms within C. goreaui cells

Following interaction with PS-MPs, there was a direct correlation between the PS-MPs' quantities and dimensions and the amounts of EPS, soluble protein, and MDA, as well as the enzymatic action of SOD in *C. goreaui* cells (Fig. 3). When exposed to PS-MPs at a particle size of 1 μm, the experimental treatment with a concentration lower than 20 mg/L had no significant impact on the EPS content in *C. goreaui* cells, while the experimental treatment with a concentration higher than 20 mg/L had a significant increase in EPS content on days 10–20 compared to that of the control group (Fig. 3A). When exposed to PS-MPs at a concentration of 20 mg/L and different particle sizes, the EPS content in *C. goreaui* cells was significantly greater on days 10–20 than that in the

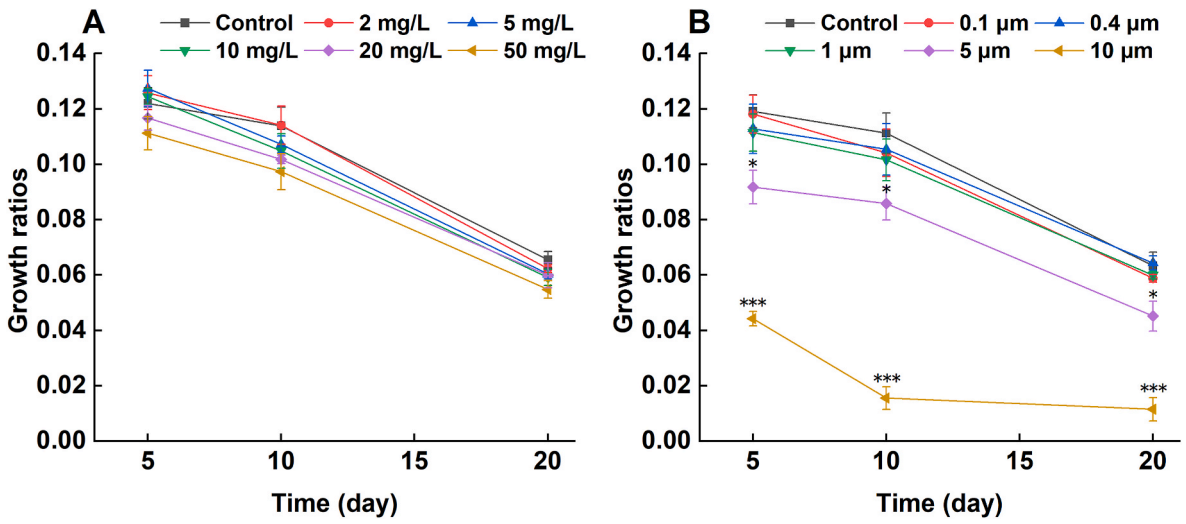

Fig. 1. The influence of PS-MPs exposure on the growth rate of *C. goreaui*. (A) Exposure to PS-MPs with different concentrations of particles with a diameter of 1 μm. (B) Exposure to PS-MPs with a concentration of 20 mg/L and different particle sizes. The data points and bars represent the mean ± the standard error (three biological replicates). The significance between the experimental group and the control group is indicated by asterisks (*: $p < 0.05$, **: $p < 0.01$, ***: $p < 0.001$).

control group (Fig. 3B), and the degree of significance was in the following order: 10 μm > 5 μm > 1 μm ≈ 0.4 μm ≈ 0.1 μm. Among the groups, the experimental group exposed to 10 μm PS-MPs had the highest degree of significance, with increases in EPS of 161.6% and 184.4% on days 10 and 20, respectively.

Upon exposure to PS-MPs with either a 20 mg/L concentration and particle sizes of 5 μm or 10 μm, or a 50 mg/L concentration with 1 μm particles, there was an alteration in the soluble protein levels in *C. goreaui* cells significantly increased on days 10–20, while the other groups showed no significant differences (Fig. 3C and D). The experimental group exposed to 10 μm PS-MPs exhibited the highest degree of significance, with increases in soluble protein of 151.6% and 190.3% on days 10 and 20, respectively.

Upon encountering PS-MPs, the alterations observed in SOD activity closely paralleled those in soluble protein levels found in *C. goreaui* cells (Fig. 3E and F). The experimental group exposed to 10 μm PS-MPs exhibited the highest degree of significance, with increases in SOD activity of 147% and 169% on days 10 and 20, respectively.

Subjecting *C. goreaui* cells to varying levels and sizes of PS-MPs particles led to a marked elevation in its MDA levels on days 10–20 of the experiment (Fig. 3G and H). Relative to the control group, the levels of MDA in the various experimental groups rose over time and exhibited a direct relationship with both the concentration and the size of the particles. Among the groups, the experimental group exposed to 10 μm PS-MPs had the greatest degree of significance, with increases in the MDA content of 261.8% and 896% on days 10 and 20, respectively.

3.3. Effects of PS-MPs exposure on the structure of C. goreaui cells

SEM analysis clearly revealed the interaction between the algal cells and the PS-MPs. When *C. goreaui* cells were exposed to PS-MPs, a large amount of PS-MPs aggregated with extracellular polysaccharides to form EPS (Fig. 4E, F, G). In the control group, the associated bacteria were in a free state and did not aggregate with *C. goreaui* (Fig. 4D), while in the experimental group, most of the associated bacteria aggregated in the EPS (Fig. 4E, F, G). Even PS-MPs with a particle size of 10 μm and a concentration of 20 mg/L caused severe wrinkling and deformation of the algal cells (Fig. 4G).

TEM observation of the damage in algal cells revealed that exposure to PS-MPs at a particle size of 10 μm and a concentration of 20 mg/L had detrimental effects on the growth of *C. goreaui*, causing cell wrinkling, dissolution of accumulations (preliminarily judged as lipids), separation of the plasma membrane, sparse fractures of the thylakoid layer, disintegration of chloroplasts, and nuclear disintegration (Fig. 5D). Furthermore, compared to those in the control group, the volume of chloroplasts in the *C. goreaui* experimental group exposed to 10 μm PS-MPs at a concentration of 20 mg/L significantly increased.

3.4. Effects of PS-MPs exposure on the transcription products of C. goreaui cells

3.4.1. Analysis of variable gene expression and Gene Ontology functional annotation in C. goreaui

Subsequent to being subjected to varying sizes and concentrations of polystyrene particles (1 μm at 10, 20, and 50 mg/L, and 10 μm at 20 mg/L), there was an observed association between the volume of upregulated genes exhibiting differential expression and the amount of PS-MPs present. In contrast, the quantity of genes showing decreased expression levels was linked to both the amount and size of the PS-MPs particles (Fig. 6A). As the concentration of PS-MPs heightened, there was an uptick in the number of downregulated differentially expressed genes, whereas the count of upregulated genes initially rose before it went on a decline. Increasing the particle size of the PS-MPs resulted in an increase in the number of downregulated differentially expressed genes (DEGs).

GO functional annotation analysis of the DEGs revealed that the effects of PS-MPs exposure on *C. goreaui* were mainly about the functions of predominantly encompassed enzyme catalysis, molecular binding, components of cells, membrane segments, metabolic functions, and cellular operations, as depicted in Fig. 6B. The impact of PS-MPs exposure on these biochemical functions was mainly manifested by the greater influence of larger particle sizes and higher concentrations (in order of significance: 10 μm-20 mg/L, 1 μm-50 mg/L, 1 μm-20 mg/L, and 1 μm-10 mg/L).

3.4.2. GO functional enrichment analysis

A further examination was carried out on the ten most markedly enhanced Gene Ontology(GO) terms associated with differentially expressed genes found within the GO enrichment analysis, as depicted in Fig. 6C. Following interaction with various particle sizes and PS-MPs concentrations, the expression of DEGs in the cohort subjected to 1 μm particles at a 20 mg/L concentration underwent upregulation. Conversely, in cohorts subjected to particle parameters of 1 μm–10 mg/L, 1 μm-50 mg/L, and 10 μm-20 mg/L, there was a predominance of downregulation in DEG numbers compared to those experiencing

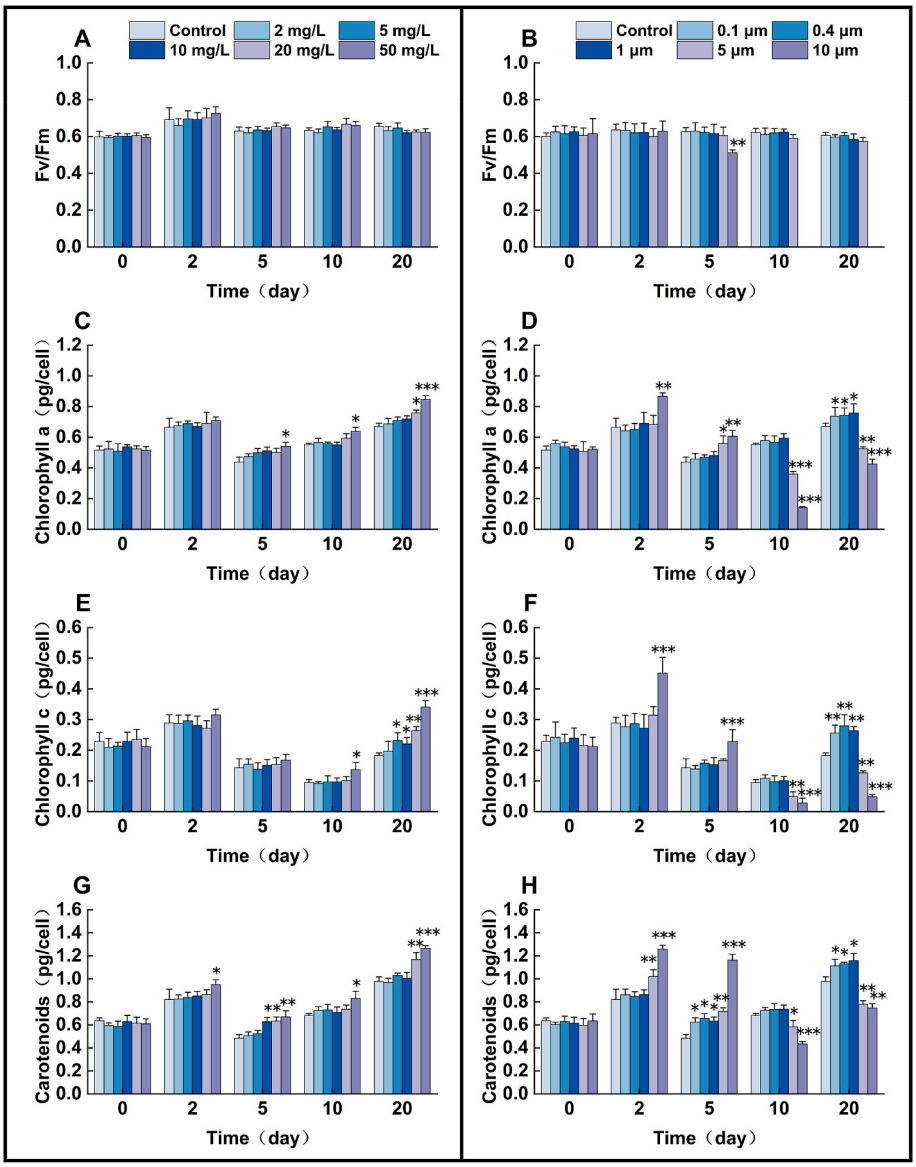

Fig. 2. Effects of PS-MPs exposure on the photosynthetic efficiency and pigment content of *C. goreaui*. (A) Exposure to PS-MPs with different concentrations of particles with a diameter of 1 μm on the Fv/Fm ratio. (B) Exposure to PS-MPs with a concentration of 20 mg/L and different particle sizes on the Fv/Fm. (C) Exposure to PS-MPs with different concentrations of particles with a diameter of 1 μm on the chlorophyll *a* concentration. (D) Exposure to PS-MPs with a concentration of 20 mg/L and different particle sizes on the chlorophyll *a* content. (E) Exposure to PS-MPs with different concentrations of particles with a diameter of 1 μm on the chlorophyll *c* content. (F) Exposure to PS-MPs with a concentration of 20 mg/L and different particle sizes on the chlorophyll *c* content. (G) Exposure to PS-MPs with different concentrations of particles with a diameter of 1 μm on the carotenoid content. (H) Exposure to PS-MPs with a concentration of 20 mg/L and different particle sizes on the carotenoid content. The bar shapes represent the mean ± the standard error (three biological replicates). The significance between the experimental group and the control group is indicated by asterisks (*: $p < 0.05$, **: $p < 0.01$, ***: $p < 0.001$).

upregulation. Among them, the experimental group exposed to a particle size of 10 μm had the highest number of downregulated DEGs, which were associated with functions such as succinate dehydrogenase activity, tetrapyrrole binding, haem binding, ionic binding, and the thylakoid lumen. Patterns of gene expression pertaining to these roles (with certain DEGs showing enrichment across various GO categories) were examined and depicted as a heatmap (refer to Fig. S1). Genes (SymbC1.scaffold2946.4) implicated in light capture and counteracting photo-oxidative stress exhibited a marked increase in expression within the experimental cohorts subjected to particle concentrations spanning 1 μm to 50 mg/L and 10 μm to 20 mg/L. Nevertheless, within the test group subjected to a particle size and a concentration of 10 μm–20 mg/L, there was also a notable elevation in the relative gene expression levels associated with the production of fatty acids (SymbC1.scaffold1086.4) and malonyl-CoA synthesis (SymbC1.scaffold6029.2, SymbC1.For scaffold5219.1, whose genes have a close association with the TCA cycle, the expression levels of the other genes were reduced.

3.4.3. KEGG pathway enrichment analysis

Fig. S2 presents the foremost 10 KEGG pathways that were markedly enriched among differentially expressed genes (DEGs) as identified by the KEGG pathway enrichment analysis. The findings suggest that the pathways most affected by various concentrations and sizes of PS-MPs pertain predominantly to metabolic functions, biosynthetic activities, and the processing of genetic information, exhibiting different degrees of involvement. Within these pathways, there was a mix of genes with increased and decreased expression levels; however, with the exception of DEGs in the group exposed to 1 μm-50 mg/L PS-MPs, the majority of DEGs exhibited decreased expression. The number of enriched DEGs in the 10 μm-20 mg/L and 1 μm-50 mg/L groups was relatively high.The

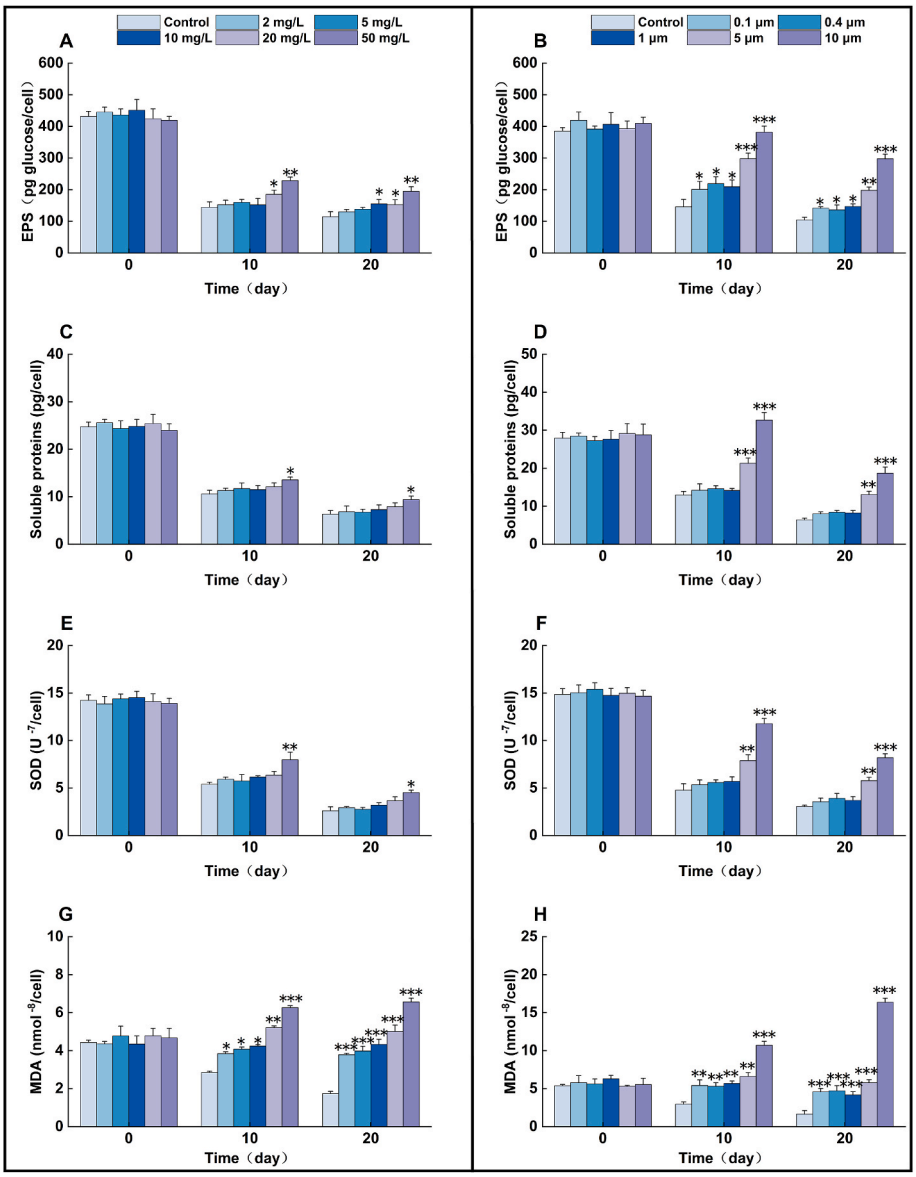

Fig. 3. Effects of PS-MPs exposure on important metabolites in *C. goreaui* cells. (A) Exposure to PS-MPs with different concentrations of particles with a diameter of 1 μm on EPS. (B) Exposure to PS-MPs with a concentration of 20 mg/L and different particle sizes on EPS. (C) Exposure to PS-MPs with different concentrations of particles with a diameter of 1 μm on soluble proteins. (D) Exposure to PS-MPs with a concentration of 20 mg/L and different particle sizes on soluble proteins. (E) Exposure to PS-MPs with different concentrations of particles with a diameter of 1 μm on SOD activity. (F) Exposure to PS-MPs with a concentration of 20 mg/L and different particle sizes on SOD activity. (G) Exposure to PS-MPs with different concentrations of particles with a diameter of 1 μm on MDA levels. (H) Exposure to PS-MPs with a concentration of 20 mg/L and different particle sizes on the MDA concentration. The bar shapes represent the mean ± the standard error (three biological replicates). The significance between the experimental group and the control group is indicated by asterisks (*: $p < 0.05$, **: $p < 0.01$, ***: $p < 0.001$).

distribution of particular gene expression within these networks (with certain differentially expressed genes being prevalent in a number of KEGG pathways) was examined and is depicted as a heatmap (refer to Fig. S3).

4. Discussion

4.1. The effect of various concentrations and sizes of PS-MPs particles on the suppression of C. goreaui growth

Although the research indicated an absence of noteworthy disparity in the growth rate of *C. goreaui* cells exposed to PS-MPs at a particle size of 1 μm or at different concentrations (0–50 mg/L), upon exposure to PS-MPs with a density of 20 mg per liter, featuring particles measuring 5 μm and 10 μm, there was a marked suppression in the proliferation of *C. goreaui*. With the most pronounced effect observed in the subset subjected to the 10-μm particles, which had decreased 62.9%–86% of the growth rate compared to the control group, nearly halted growth entirely. This indicated that larger PS-MPs particle sizes have a greater impact on the growth of *C. goreaui*. Similarly, Liu et al. (2019) reported that when *Scenedesmus obliquus* was exposed to PS-MPs at a concentration of 75 mg/L, the inhibitory effect on growth was significantly greater for 0.5 μm particles than for 0.1 μm particles. Xiao et al. (2020) also reported that at a concentration of 10 mg/L, the toxicity of 5 μm particles on *Euglena gracilis* growth was greater than that of 0.1 μm particles. In addition, through SEM, this study revealed that PS-MPs of different sizes all aggregated with *C. goreaui* to form EPS, and the larger particle size group formed more EPS than the smaller particle size group. The group of 10 μm–20 mg/L caused cell shrinkage and deformation. However, Cao et al. (2022b) reported that smaller PS-MPs (1 μm) were

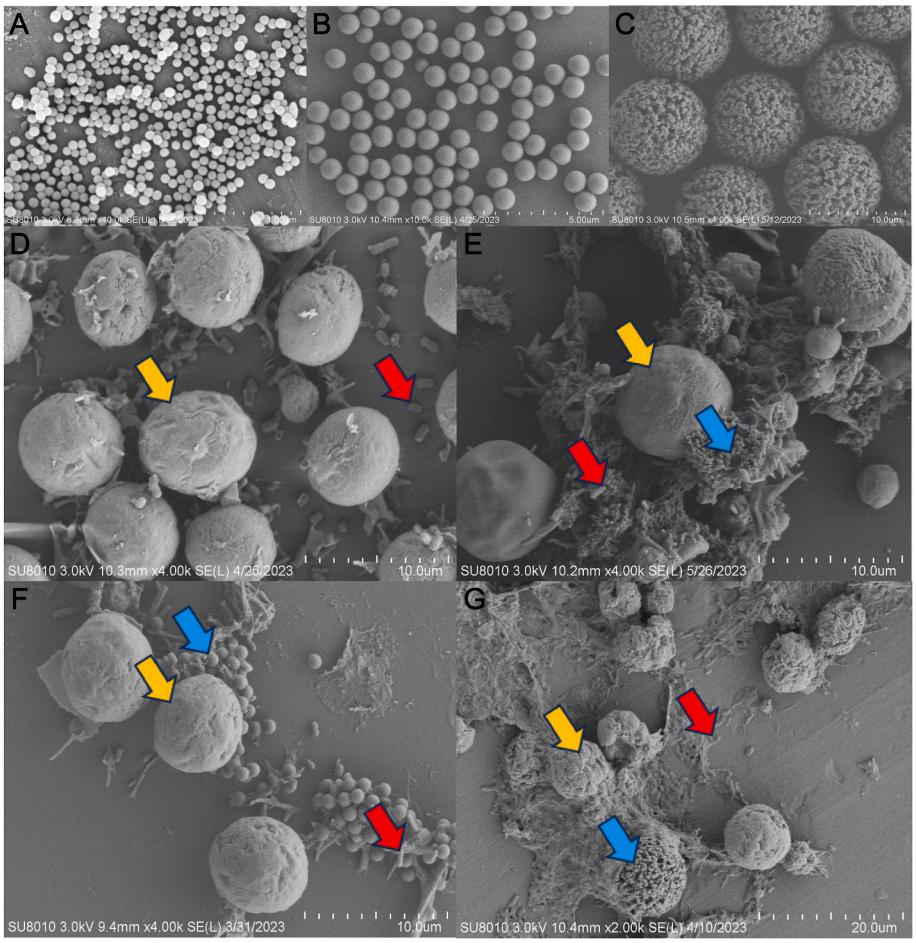

Fig. 4. Effects of PS-MPs exposure on the surface structure of *C. goreaui* cells. (A) PS-MPs with a particle size of 0.1 μm. (B) PS-MPs with a particle size of 1 μm. (C) PS-MPs with a particle size of 10 μm. (D) Control group. (E) Exposure group with a particle size of 0.1 μm and a concentration of 20 mg/L. (F) Exposure group with a particle size of 1 μm and a concentration of 20 mg/L. (G) Exposure group with a particle size of 10 μm and a concentration of 20 mg/L. Yellow arrows point to *C. goreaui* cells, red arrows point to associated bacteria, and blue arrows point to PS-MPs. (For interpretation of the references to colour in this figure legend, the reader is referred to the Web version of this article.)

more likely to interact with *C. pyrenoidosa* and form EPS on the cell surface, while PS-MPs particles with a size of 5 μm did not aggregate with *C. pyrenoidosa* cells to form EPS. This indicates that the impact of PS-MPs on marine microalgae is species specific. Therefore, when exploring the toxic effects of MPs on marine microalgae, it is necessary to carefully consider the differences in response of different microalgae species to MPs. Algal cells excrete EPS into their surrounding milieu, which are crucial for their development and intrinsic defense mechanisms (Li et al., 2020). When PS-MPs aggregate with algal cells to form a large amount of EPS, they can block light and affect the photosynthesis of algal cells, causing severe oxidative damage to the cells (Chen et al., 2012). Furthermore, this study revealed that the increase in EPS caused by PS-MPs exposure also affected the growth of bacteria associated with *C. goreaui*, thereby impacting the growth of *C. goreaui*.

4.2. Stress regulation of photosynthetic pigments in C. goreaui after PS-MPs exposure

When the available light energy for cells decreases, the chlorophyll content increases to maintain photosynthesis (Falkowski and Owens, 1980). During the chill of winter, the symbiotic algae housed within corals transition from a simple layer structure to a more complex, stratified configuration, enhancing their ability to absorb light, which consequently raises both the concentration and the chlorophyll concentration in these algae, as reported by (Venn et al., 2008). Conversely, in the summer months, characterized by greater warmth and more intense sunlight, there is a reduction in both the concentration and chlorophyll levels of the symbiotic algae. These findings indicate that symbiotic algae regulate their own chlorophyll content to maintain stable photosynthesis. During the PS-MPs exposure experiments, *C. goreaui* also employed similar stress strategies. The chlorophyll *a* content in *C. goreaui* cells significantly increased on the 7th day of exposure to PS-MPs at a particle size and concentration ranging from 1 μm to 5 mg/L, while the photochemical efficiency remained stable throughout the exposure experiment (Su et al., 2020). This study revealed that, during the initial stage of PS-MPs exposure, *C. goreaui* cells adjust their content of photosynthetic pigments to maintain stable photosynthesis. In the experimental groups exposed to larger particles (5 μm-20 mg/L and 10 μm-20 mg/L), the contents of pigment in *C. goreaui* cells significantly increased in the early stage of exposure (0–5 days), indicating a positive response from the algal cells. However, due to the stronger damaging effect of larger PS-MPs on *C. goreaui*, following the fifth day, there was a notable reduction in the pigment concentration within the algal cells. Thus it can be seen that when the particle size of PS-MPs exceeds 5 μm, the chloroplast function of *C. goreaui* is impaired. Furthermore, cell structure analysis also revealed that *C. goreaui* cells exhibited severe damage, such as cell contraction and chloroplast disintegration, in the exposure experiment at a particle size and concentration of 10 μm–20 mg/L, leading to weakened photosynthesis. The synthesis of photosynthetic pigments is directly related to tetrapyrrole

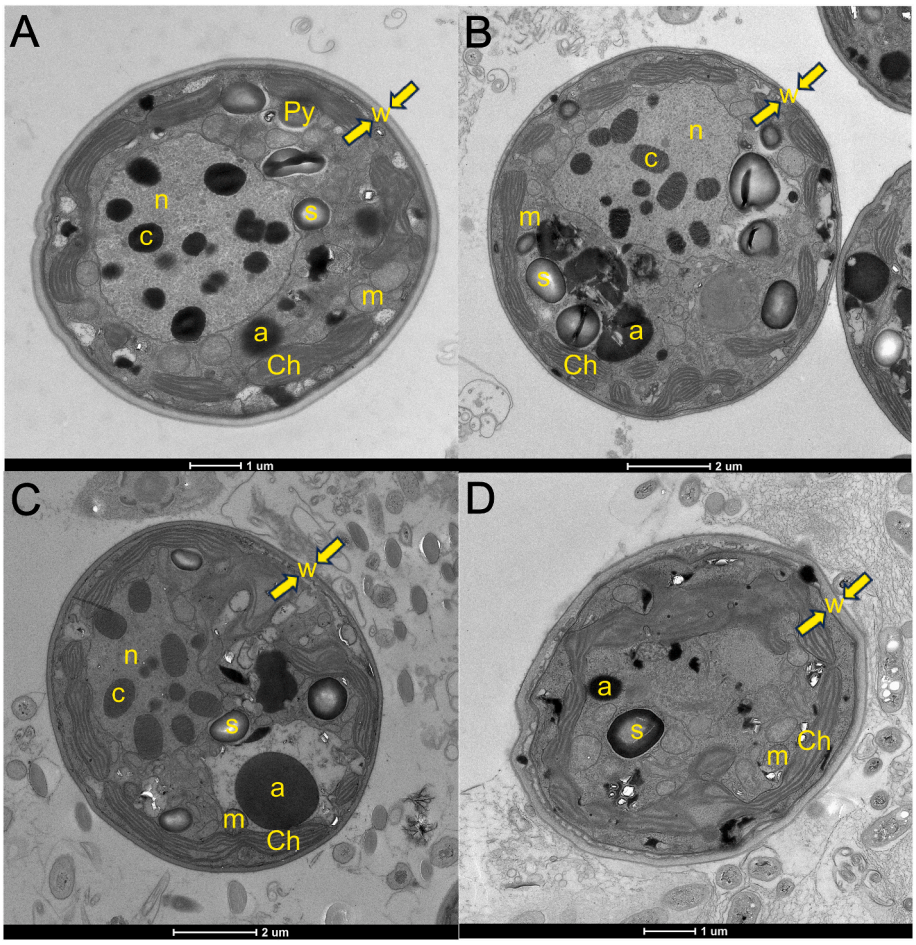

Fig. 5. Effects of PS-MPs exposure on the internal structure of *C. goreaui* cells. (A) Control group. (B) Exposure group with a particle size of 0.1 μm and a concentration of 20 mg/L. (C) Exposure group with a particle size of 1 μm and a concentration of 20 mg/L. (D) Exposure group with a particle size of 10 μm and a concentration of 20 mg/L "n": nucleus; "c": chromosome; "Ch": chloroplast; "Py": pyrenoid; "m": mitochondrion; "s": starch; "a": accumulation body; "w": cell wall.

binding and haem binding (Ikeuchi and Ishizuka, 2008; Xiao et al., 2023), and these dual functions are based on ionic binding. During the experiment involving exposure to PS-MPs, genomic investigation demonstrated a notable decrease in the expression of genes associated with these activities within the group subjected to particles varying in size from 10 μm and having a concentration up to 20 mg/L, suggesting a diminished synthesis of photosynthetic pigments followed by a reduction in the ability to perform photosynthesis. And the significant downregulation of gene expression related to chloroplast thylakoid lumina indicates that chloroplast function is inhibited.

4.3. Exposure to PS-MPs induces oxidative stress and incurs oxidative damage in C. goreaui

Succinate dehydrogenase is one of the key components connecting oxidative phosphorylation and electron transfer, providing electrons for aerobic respiration and energy production in eukaryotic mitochondria and various prokaryotic cells (Lussey-Lepoutre et al., 2015). Haem binding also plays an important role in cellular respiration and energy metabolism (Khan and Quigley, 2011; Xiao et al., 2023). In the PS-MPs exposure experiment, transcriptomic analysis revealed significant downregulation of gene expression related to Succinate dehydrogenase activity, haem, and ionic binding in the experimental group with particle size and concentration of 10 μm–20 mg/L (Fig. 6C), indicating insufficient energy supply and inhibited metabolism. During this process, *C. goreaui* cell growth is restricted, and metabolism is disrupted. Due to its photosynthetic autotrophic nature, *C. goreaui* accumulated energy substances such as sugars and proteins through photosynthesis during cultivation. And the MDA produced by oxidation reaction will also increase with the increase of cell number. As the exposure days increased, the total metabolite content in the control group gradually accumulated, however, as the number of cells increases, their single-cell content gradually decreases, which is consistent with the results of other researchers (Li et al., 2020; Cao et al., 2022b).

Soluble proteins are important nutrients and osmoregulatory substances in cells that not only contribute to the improvement of cell water-holding capacity but also protect biomacromolecules and biomembranes in cells (Guzmán-Murillo et al., 2007; Qian et al., 2008). When exposed to relatively high concentrations (1 μm-50 mg/L) and large particle sizes (5 μm-20 mg/L and 10 μm-20 mg/L) of PS-MPs, the markedly higher presence of the content of soluble proteins in *C. goreaui* cells compared to the control group could be associated with the algae's innate self-repair and defense capabilities. The content of soluble proteins in *C. goreaui* cells increased with increasing PS-MPs particle size, indicating that larger PS-MPs particles (5 μm and 10 μm) cause more severe damage to algal cells and produce stronger stress responses.

When PS-MPs exposure leads to the inhibition of photosynthesis and insufficient energy supply in *C. goreaui*, the electron transfer rate decreases, resulting in electron accumulation and increased generation of reactive oxygen species (ROS) (Cao et al., 2022a). Upon suffering extensive harm to their cellular structures and internal components due to ROS, cells activate their innate defense mechanisms to synthesize protective enzymes like catalase (CAT), superoxide dismutase (SOD), and peroxidase (POD), with the objective of mitigating the detrimental

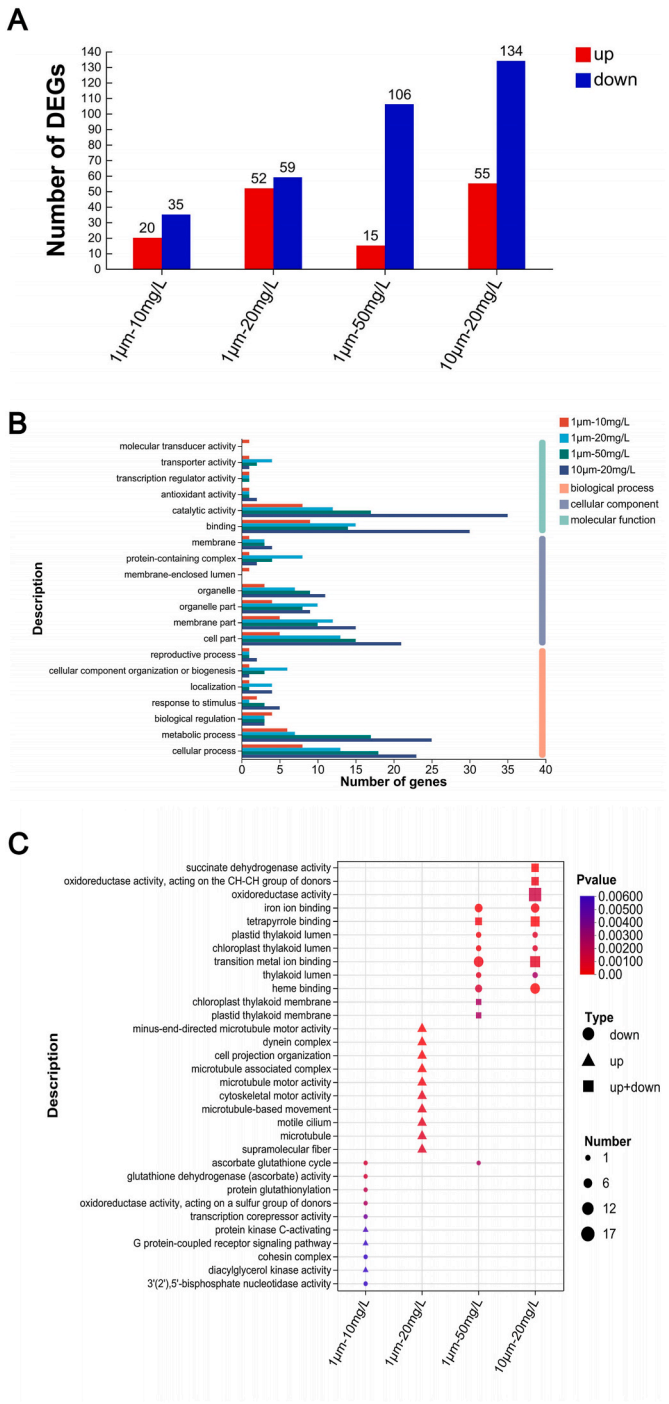

Fig. 6. Effects of PS-MPs exposure on the transcription products. (A) Difference statistics for the Number of total DEGs. (B) GO functional annotation analysis. (C) Bubble chart of multi-gene set GO enrichment analysis.

impact of these reactive molecules (Cao et al., 2015). In the present study, when different-sized PS-MPs (1 μm at 50 mg/L, 5 μm at 20 mg/L, and 10 μm at 20 mg/L) were administered to the *C. goreaui*, resulting in a marked elevation in the SOD activity within the algal cells compared to the control group. This suggests an increase in ROS generation in the cells, with the SOD activity showing a direct relationship to the PS-MPs particle size. These findings suggested that larger PS-MPs particles have stronger toxic effects on *C. goreaui*, leading to the production of more ROS in the cells.

The substance MDA, which results from the peroxidation of membrane lipids, serves as an indicator of the extent of oxidative harm (Qian et al., 2008; Melegari et al., 2012). Excessive ROS exacerbates cell membrane lipid peroxidation, resulting in the production of a large amount of MDA (Melegari et al., 2012; Xiao et al., 2020). Upon subjecting *C. goreaui* cells to various levels and sizes of PS-MPs, there was a notable increase in MDA levels compared to the control group. Additionally, it was observed that an upsurge in both the amount and dimensions of the particles led to an enhanced accumulation of MDA, signifying intensified oxidative harm.

4.4. Considerations on the use of higher concentrations of MPs in experimental design

In marine environments, the toxicological effects of MPs are a prolonged process. In this study, we employed higher concentrations of MPs to investigate their impact on key symbiotic microorganisms of corals, with the aim of exploring the potential threats posed by MPs to coral reef ecosystems. As indicated by similar studies, utilizing higher concentrations of MPs in short-term acute exposure experiments provides clearer insights into their potential impacts (Mao et al., 2018; Li et al., 2020; Cui et al., 2022; Khatiwada et al., 2023). It is undeniable that using higher concentrations of MPs to explore their toxicological effects has certain limitations. However, due to the current inadequacies in detection methods for microplastic concentrations at micron and nanoscale levels in natural environments, the measured values may be lower than the actual values. Moreover, the global production and discharge of plastic products are still increasing, and large particles of plastic are further decomposed into small particle size MPs (Thompson et al., 2004; Lambert et al., 2013; Auta et al., 2017; Yang et al., 2020). As such, the experimental findings of this study provide valuable insights into the impacts of MPs on coral reef ecosystems to some extent.

5. Conclusion

This research indicated harmful impacts of PS-MPs on *C. goreaui*, and the impacts are closely related to particle size, with larger particles exhibiting greater toxicity. Specifically, PS-MPs aggregate with *C. goreaui* cells to form a large amount of EPS, which blocks light and inhibits photosynthesis, significantly increases the ROS content, and causes structural damage to *C. goreaui* cells. In addition, PS-MPs inhibited the expression of genes related to photosynthesis and cellular metabolism in *C. goreaui* cells. Overall, based on the toxic effects of PS-MPs on the common coral symbiont Symbiodiniaceae (*C. goreaui*) and the importance of Symbiodiniaceae to coral, MPs pollution is presumed to pose a potential threat to coral reef ecosystems. Due to the difficulty of degrading MPs in the natural environment and the continuous increase in plastic waste emissions, if not controlled, future plastic pollution will inevitably severely damage coral reef ecosystems.

CRediT authorship contribution statement

Jiayuan Liang: Writing – review & editing, Writing – original draft, Validation, Resources, Project administration, Methodology, Investigation, Formal analysis, Data curation, Conceptualization. **Tianyi Niu:** Writing – review & editing, Writing – original draft, Visualization, Validation, Software, Methodology, Investigation, Data curation. **Li Zhang:** Writing – review & editing, Supervision, Formal analysis. **Yating Yang:** Software, Methodology. **Zhicong Li:** Visualization, Validation, Supervision. **Zhuqing Liang:** Writing – review & editing, Validation, Investigation. **Kefu Yu:** Writing – review & editing, Supervision, Resources, Project administration, Funding acquisition, Conceptualization. **Sanqiang Gong:** Visualization, Software, Methodology.

Data availability

The data generated as part of this study are available upon request.

The raw sequence data (a total of 15 RNA sequencing libraries) produced in this study were deposited in the Sequence Read Archive (PRJNA1056117) of the NCBI (https://blast.ncbi.nlm.nih.gov).

Declaration of competing interest

The authors declare the following financial interests/personal relationships which may be considered as potential competing interests: Jiayuan Liang reports financial support was provided by the National Natural Science Foundation of China. If there are other authors, they declare that they have no known competing financial interests or personal relationships that could have appeared to influence the work reported in this paper.

Acknowledgements

This work was supported by the National Natural Science Foundation of China (42030502 and 42090041), the Self-Topic Project of Guangxi Laboratory on the Study of Coral Reefs in the South China Sea (GXLSCRSCS2023101), and the Science and Technology Project of Guangxi (Nos. AD17129063 and AA17204074).

Appendix A. Supplementary data

Supplementary data to this article can be found online at https://doi.org/10.1016/j.envres.2025.120750.

Data availability

Data will be made available on request.

References

Ali, A., Kriefall, N.G., Emery, L.E., Kenkel, C.D., Matz, M.V., Davies, S.W., 2019. Recruit symbiosis establishment and Symbiodiniaceae composition influenced by adult corals and reef sediment. Coral Reefs 38, 405–415.

Auta, H., Emenike, C., Fauziah, S., 2017. Screening of Bacillus strains isolated from mangrove ecosystems in Peninsular Malaysia for microplastic degradation. Environ. Pollut. 231, 1552–1559.

Baker, D.M., Andras, J.P., Jordán-Garza, A.G., Fogel, M.L., 2013. Nitrate competition in a coral symbiosis varies with temperature among Symbiodinium clades. ISME J. 7 (6), 1248–1251.

Cao, D.-j., Shi, X.-d., Li, H., Xie, P.-p., Zhang, H.-m., Deng, J.-w., Liang, Y.-g., 2015. Effects of lead on tolerance, bioaccumulation, and antioxidative defense system of green algae, Cladophora. Ecotoxicol. Environ. Saf. 112, 231–237.

Cao, Q., Jiang, Y., Yang, H., Zhang, Y., Wei, W., 2022a. Comprehensive toxic effects of povidone iodine on microalgae *Chlorella pyrenoidosa* under different concentrations. Aquacult. Res. 53 (5), 1833–1841.

Cao, Q., Sun, W., Yang, T., Zhu, Z., Jiang, Y., Hu, W., Wei, W., Zhang, Y., Yang, H., 2022b. The toxic effects of polystyrene microplastics on freshwater algae *Chlorella pyrenoidosa* depends on the different size of polystyrene microplastics. Chemosphere 308, 136135.

Chen, P., Powell, B.A., Mortimer, M., Ke, P.C., 2012. Adaptive interactions between zinc oxide nanoparticles and *Chlorella sp.* Environ. Sci. Technol. 46 (21), 12178–12185.

Chen, Y., Ling, Y., Li, X., Hu, J., Cao, C., He, D., 2020. Size-dependent cellular internalization and effects of polystyrene microplastics in microalgae *P. helgolandica var. tsingtaoensis* and *S. quadricauda*. J. Hazard Mater. 399, 123092.

Cui, Y., Liu, M., Selvam, S., Ding, Y., Wu, Q., Pitchaimani, V.S., Huang, P., Ke, H., Zheng, H., Liu, F., 2022. Microplastics in the surface waters of the South China sea and the western Pacific Ocean: different size classes reflecting various sources and transport. Chemosphere 299, 134456.

Ding, J., Jiang, F., Li, J., Wang, Z., Sun, C., Wang, Z., Fu, L., Ding, N.X., He, C., 2019a. Microplastics in the coral reef systems from xisha islands of South China sea. Environ. Sci. Technol. 53 (14), 8036–8046.

Ding, J., Li, J., Sun, C., Jiang, F., Ju, P., Qu, L., Zheng, Y., He, C., 2019b. Detection of microplastics in local marine organisms using a multi-technology system. Anal. Methods 11 (1), 78–87.

Falkowski, P.G., Owens, T.G., 1980. Light—shade adaptation: two strategies in marine phytoplankton. Plant Physiol. 66 (4), 592–595.

Gong, S., Chai, G., Sun, W., Zhang, F., Yu, K., Li, Z., 2021. Global-scale diversity and distribution characteristics of reef-associated symbiodiniaceae via the cluster-based parsimony of internal transcribed spacer 2 sequences. J. Ocean Univ. China 20, 296–306.

González-Pech, R.A., Bhattacharya, D., Ragan, M.A., Chan, C.X., 2019. Genome evolution of coral reef symbionts as intracellular residents. Trends Ecol. Evol. 34 (9), 799–806.

Guzmán-Murillo, M.A., López-Bolaños, C.C., Ledesma-Verdejo, T., Roldan-Libenson, G., Cadena-Roa, M.A., Ascencio, F., 2007. Effects of fertilizer-based culture media on the production of exocellular polysaccharides and cellular superoxide dismutase by Phaeodactylum tricornutum (Bohlin). J. Appl. Phycol. 19, 33–41.

Hoegh-Guldberg, O., 2011. Coral reef ecosystems and anthropogenic climate change. Reg. Environ. Change 11, 215–227.

Houlbrèque, F., Ferrier-Pagès, C., 2009. Heterotrophy in tropical scleractinian corals. Biol. Rev. 84 (1), 1–17.

Huang, Y., Yan, M., Xu, K., Nie, H., Gong, H., Wang, J., 2019. Distribution characteristics of microplastics in zhubi reef from South China sea. Environ. Pollut. 255, 113133.

Hughes, T.P., Baird, A.H., Bellwood, D.R., Card, M., Connolly, S.R., Folke, C., Grosberg, R., Hoegh-Guldberg, O., Jackson, J.B., Kleypas, J., 2003. Climate change, human impacts, and the resilience of coral reefs. Science 301 (5635), 929–933.

Ikeuchi, M., Ishizuka, T., 2008. Cyanobacteriochromes: a new superfamily of tetrapyrrole-binding photoreceptors in cyanobacteria. Photochem. Photobiol. Sci. 7 (10), 1159–1167.

Imhof, H.K., Sigl, R., Brauer, E., Feyl, S., Giesemann, P., Klink, S., Leupolz, K., Löder, M. G., Löschel, L.A., Missun, J., 2017. Spatial and temporal variation of macro-, meso- and microplastic abundance on a remote coral island of the Maldives, Indian Ocean. Mar. Pollut. Bull. 116 (1–2), 340–347.

Ivleva, N.P., Wiesheu, A.C., Niessner, R., 2017. Microplastic in aquatic ecosystems. Angew. Chem. Int. Ed. 56 (7), 1720–1739.

Jambeck, J.R., Geyer, R., Wilcox, C., Siegler, T.R., Perryman, M., Andrady, A., Narayan, R., Law, K.L., 2015. Plastic waste inputs from land into the ocean. Science 347 (6223), 768–771.

Jensen, L.H., Motti, C.A., Garm, A.L., Tonin, H., Kroon, F.J., 2019. Sources, distribution and fate of microfibres on the Great barrier reef, Australia. Sci. Rep. 9 (1), 9021.

Khan, A.A., Quigley, J.G., 2011. Control of intracellular heme levels: heme transporters and heme oxygenases. Biochim. Biophys. Acta Mol. Cell Res. 1813 (5), 668–682.

Khatiwada, J.R., Madsen, C., Warwick, C., Shrestha, S., Chio, C., Qin, W., 2023. Interaction between polyethylene terephthalate (PET) microplastic and microalgae (Scenedesmus spp.): effect on the growth, chlorophyll content, and hetero-aggregation. Environ. Adv. 13, 100399.

Kor, K., Mehdinia, A., 2020. Neustonic microplastic pollution in the Persian Gulf. Mar. Pollut. Bull. 150, 110665.

LaJeunesse, T.C., Parkinson, J.E., Gabrielson, P.W., Jeong, H.J., Reimer, J.D., Voolstra, C.R., Santos, S.R., 2018. Systematic revision of Symbiodiniaceae highlights the antiquity and diversity of coral endosymbionts. Curr. Biol. 28 (16), 2570, 2580. e2576.

Lambert, S., Sinclair, C.J., Bradley, E.L., Boxall, A.B., 2013. Effects of environmental conditions on latex degradation in aquatic systems. Sci. Total Environ. 447, 225–234.

Li, C., Wang, X., Liu, K., Zhu, L., Wei, N., Zong, C., Li, D., 2021a. Pelagic microplastics in surface water of the Eastern Indian Ocean during monsoon transition period: abundance, distribution, and characteristics. Sci. Total Environ. 755, 142629.

Li, J., Ouyang, Z., Liu, P., Zhao, X., Wu, R., Zhang, C., Lin, C., Li, Y., Guo, X., 2021b. Distribution and characteristics of microplastics in the basin of Chishui river in Renhuai, China. Sci. Total Environ. 773, 145591.

Li, S., Wang, P., Zhang, C., Zhou, X., Yin, Z., Hu, T., Hu, D., Liu, C., Zhu, L., 2020. Influence of polystyrene microplastics on the growth, photosynthetic efficiency and aggregation of freshwater microalgae Chlamydomonas reinhardtii. Sci. Total Environ. 714, 136767.

Liu, G., Jiang, R., You, J., Muir, D.C., Zeng, E.Y., 2019. Microplastic impacts on microalgae growth: effects of size and humic acid. Environ. Sci. Technol. 54 (3), 1782–1789.

Lussey-Lepoutre, C., Hollinshead, K.E., Ludwig, C., Menara, M., Morin, A., Castro-Vega, L.-J., Parker, S.J., Janin, M., Martinelli, C., Ottolenghi, C., 2015. Loss of succinate dehydrogenase activity results in dependency on pyruvate carboxylation for cellular anabolism. Nat. Commun. 6 (1), 8784.

Mao, Y., Ai, H., Chen, Y., Zhang, Z., Zeng, P., Kang, L., Li, W., Gu, W., He, Q., Li, H., 2018. Phytoplankton response to polystyrene microplastics: perspective from an entire growth period. Chemosphere 208, 59–68.

Marangoni, L.F., Beraud, E., Ferrier-Pagès, C., 2022. Polystyrene nanoplastics impair the photosynthetic capacities of Symbiodiniaceae and promote coral bleaching. Sci. Total Environ. 815, 152136.

Melegari, S.P., Perreault, F., Moukha, S., Popovic, R., Creppy, E.E., Matias, W.G., 2012. Induction to oxidative stress by saxitoxin investigated through lipid peroxidation in Neuro 2A cells and Chlamydomonas reinhardtii alga. Chemosphere 89 (1), 38–43.

Mooney, H., Larigauderie, A., Cesario, M., Elmquist, T., Hoegh-Guldberg, O., Lavorel, S., Mace, G.M., Palmer, M., Scholes, R., Yahara, T., 2009. Biodiversity, climate change, and ecosystem services. Curr. Opin. Environ. Sustain. 1 (1), 46–54.

Ng, T.Y., Chui, A.P.Y., Ang, P., 2019. Onset of symbiosis in planula larvae of scleractinian corals. Hydrobiologia 842 (1), 113–126.

Qian, H., Chen, W., Sheng, G.D., Xu, X., Liu, W., Fu, Z., 2008. Effects of glufosinate on antioxidant enzymes, subcellular structure, and gene expression in the unicellular green alga Chlorella vulgaris. Aquat. Toxicol. 88 (4), 301–307.

Qin, L., Xu, Y., Chen, J., Niu, T., Yu, K., Liang, J., 2023. Optimization of in vitro culture method for zooxanthellae associated with reef-building corals. Acta Microbiol. Sin. 63 (4), 1658–1671. https://doi.org/10.13343/j.cnki.wsxb.20220656.

Reaka-Kudla, L, M., 1997. The global biodiversity of coral reefs: a comparison with rain forests. Biodiversity II: Understanding and protecting our biological resources 2, 551.

Ripken, C., Khalturin, K., Shoguchi, E., 2020. Response of coral reef dinoflagellates to nanoplastics under experimental conditions. bioRxiv 2020, 2009. 2023.310847.

Ritchie, R.J., 2006. Consistent sets of spectrophotometric chlorophyll equations for acetone, methanol and ethanol solvents. Photosynth. Res. 89, 27–41.

Robbins, S.J., Singleton, C.M., Chan, C.X., Messer, L.F., Geers, A.U., Ying, H., Baker, A., Bell, S.C., Morrow, K.M., Ragan, M.A., 2019. A genomic view of the reef-building coral Porites lutea and its microbial symbionts. Nat Microbiol 4, 2090–2100.
Rotjan, R.D., Sharp, K.H., Gauthier, A.E., Yelton, R., Lopez, E.M.B., Carilli, J., Kagan, J. C., Urban-Rich, J., 2019. Patterns, dynamics and consequences of microplastic ingestion by the temperate coral, Astrangia poculata. Proceedings of the Royal Society B 286 (1905), 20190726.
Saliu, F., Montano, S., Garavaglia, M.G., Lasagni, M., Seveso, D., Galli, P., 2018. Microplastic and charred microplastic in the Faafu Atoll, Maldives. Mar. Pollut. Bull. 136, 464–471.
Sana, S.S., Dogiparthi, L.K., Gangadhar, L., Chakravorty, A., Abhishek, N., 2020. Effects of microplastics and nanoplastics on marine environment and human health. Environ. Sci. Pollut. Control Ser. 27, 44743–44756.
Schwarz, A., Ligthart, T., Boukris, E., Van Harmelen, T., 2019. Sources, transport, and accumulation of different types of plastic litter in aquatic environments: a review study. Mar. Pollut. Bull. 143, 92–100.
Sendra, M., Pereiro, P., Yeste, M.P., Mercado, L., Figueras, A., Novoa, B., 2021. Size matters: Zebrafish (Danio rerio) as a model to study toxicity of nanoplastics from cells to the whole organism. Environ. Pollut. 268, 115769.
Su, Y., Zhang, K., Zhou, Z., Wang, J., Yang, X., Tang, J., Li, H., Lin, S., 2020. Microplastic exposure represses the growth of endosymbiotic dinoflagellate *Cladocopium goreaui* in culture through affecting its apoptosis and metabolism. Chemosphere 244, 125485.
Sun, Y., 2020. Studies on Physiological Response and Omics Analysis of Early Development of Tow Reff Corals to Ocean Warming and Acidification. University of Chinese Academy of Sciences, Doctor.
Tang, J., Ni, X., Zhou, Z., Wang, L., Lin, S., 2018. Acute microplastic exposure raises stress response and suppresses detoxification and immune capacities in the scleractinian coral Pocillopora damicornis. Environ. Pollut. 243, 66–74.
Thompson, R.C., Olsen, Y., Mitchell, R.P., Davis, A., Rowland, S.J., John, A.W., McGonigle, D., Russell, A.E., 2004. Lost at sea: where is all the plastic? Science 304 (5672), 838-838.
Van Sebille, E., Aliani, S., Law, K.L., Maximenko, N., Alsina, J.M., Bagaev, A., Bergmann, M., Chapron, B., Chubarenko, I., Cózar, A., 2020. The physical oceanography of the transport of floating marine debris. Environ. Res. Lett. 15 (2), 023003.
Venn, A.A., Loram, J.E., Douglas, A.E., 2008. Photosynthetic symbioses in animals. J. Exp. Bot. 59 (5), 1069–1080.
Wegley, L., Edwards, R., Rodriguez-Brito, B., Liu, H., Rohwer, F., 2007. Metagenomic analysis of the microbial community associated with the coral Porites astreoides. Environ. Microbiol. 9 (11), 2707–2719.
Wright, S.L., Thompson, R.C., Galloway, T.S., 2013. The physical impacts of microplastics on marine organisms: a review. Environ. Pollut. 178, 483–492.
Xiao, X., Li, W., Li, S., Zuo, X., Liu, J., Guo, L., Lu, X., Zhang, L., 2023. The growth inhibition of polyethylene nanoplastics on the bait-microalgae isochrysis galbana based on the transcriptome analysis. Microorganisms 11 (5), 1108.
Xiao, Y., Jiang, X., Liao, Y., Zhao, W., Zhao, P., Li, M., 2020. Adverse physiological and molecular level effects of polystyrene microplastics on freshwater microalgae. Chemosphere 255, 126914.
Yang, H., Xiong, H., Mi, K., Xue, W., Wei, W., Zhang, Y., 2020. Toxicity comparison of nano-sized and micron-sized microplastics to Goldfish Carassius auratus Larvae. J. Hazard Mater. 388, 122058.
Yu, K., 2012. Coral reefs in the South China Sea: their response to and records on past environmental changes. Sci. China Earth Sci. 42 (8), 1160–1172.
Yu, K., 2018. Introduction to the Science of Coral Reefs, first ed. Science Press, Beijing.
Yue, F., Zhang, J., Xu, J., Niu, T., Lü, X., Liu, M., 2022. Effects of monosaccharide composition on quantitative analysis of total sugar content by phenol-sulfuric acid method. Front. Nutr. 9, 963318.
Zhou, Z., Zhang, P., Zhang, G., Wang, S., Cai, Y., Wang, H., 2021. Vertical microplastic distribution in sediments of Fuhe river estuary to Baiyangdian Wetland in northern China. Chemosphere 280, 130800.